Plant-Derived MINA-05 Inhibits Human Prostate Cancer Proliferation *In Vitro* and Lymph Node Spread *In Vivo*[1]

Kate Vandyke[*,†], *Melanie Y. White*[‡], *Terry Nguyen-Khuong*[‡], *Kim Ow*[*,†], *Sharon C.-W. Luk*[§], *Elizabeth A. Kingsley*[*,†], *Alexandra Rowe*[*,†], *Shiu-Fun Pang*[§], *Bradley J. Walsh*[‡] *and Pamela J. Russell*[*,†]

*Oncology Research Centre, Prince of Wales Hospital, Barker Street, Randwick, NSW 2031, Australia; [†]Department of Clinical Medicine, University of New South Wales, Sydney, NSW 2052, Australia; [‡]Minomic Pty Ltd, PO Box 664, Harbord, NSW 2096, Australia; [§]CK Life Sciences Int'l Inc., 2 Dai Fu Street, Tai Po Industrial Estate, Hong Kong

Abstract

Few treatment options exist for metastatic prostate cancer (PC) that becomes hormone refractory (HRPC). *In vitro*, plant-derived MINA-05 caused dose-dependent decreases in cell numbers in HRPC cell lines LNCaP-C4-2B and PC-3, and in androgen-sensitive LNCaP-FGC, DuCaP, and LAPC-4, by WST-1 assay. MINA-05 pre-treatment significantly decreased clonogenic survival in agar and on plastic at 1 × and 2 × IC_{50} for PC-3 (*P < .05* and *P < .001*, respectively), and at $\frac{1}{2}$ ×, 1 ×, and 2 × IC_{50} for LNCaP-FGC cells (*P < .001*). MINA-05 also induced G_2M arrest of LNCaP-FGC and PC-3 cells (by flow cytometry) and caused some apoptosis in LNCaP-FGC (sub-G_1 peak on flow, expression of activated caspase-3) but not in PC-3 cells. Western blotting indicated that these cell cycle changes were associated with decreased levels of regulatory proteins cyclin B1 and cdc25C. MINA-05 given daily by gavage for 39 days did not diminish primary orthotopic PC-3 growth in nude mice, but decreased the extent of lymph node invasion at higher doses. We conclude that MINA-05 induces G_2M arrest, inhibits cell growth, reduces PC cell regrowth *in vitro*, and reduces lymph node invasion after orthotopic PC-3 cell implantation *in vivo*. It has potential as an adjuvant treatment for patients with PC.

Neoplasia (2007) **9,** 322–331

Keywords: Prostate cancer, G_2M block, MINA-05 herbal treatment, lymph node metastases, clonogenic assays.

Introduction

Prostate cancer (PC) is currently the second highest killer of Occidental men from cancer [1]. PC commonly metastasizes to lymph nodes and bone and, once regional lymph node involvement occurs, 85% of patients will develop distant metastases within 5 years with a median survival time of 1 to 3 years (http://www.cancer.gov/cancertopics/pdq/treatment/prostate/healthprofessional). Metastatic disease is primarily treated by androgen ablation but recurs as hormone-refractory PC (HRPC). Chemotherapy for such patients is mostly palliative; new therapeutic strategies are needed. Complementary therapies are used by up to 80% of patients with cancer [2], emphasizing the need to delineate their mechanisms of action, pharmacology, and toxicology [3].

Treatment with MINA-05, a plant extract developed by CK Life Sciences Int'l Inc. (Hong Kong), has been shown to inhibit the growth of subcutaneous PC-3 tumors in athymic nude mice (Liu et al., personal communication). MINA-05 contains Wu Wei Zi (*Schisandra chinensis*), soybean (*Glycine max*), Gua Lou (*Trichosanthes kirilowii* Maxim), and yucca (*Yucca schidigera*), ingredients shown to induce cell cycle arrest. *S. chinensis* induces apoptosis of PC cells by inhibiting androgen receptor expression [4]. Genistein, daidzein, and isoflavonoids in soybean have potential for breast cancer prevention [5], and genistein induces G_2M arrest in MCF-7 cells [6]. In addition, dietary genistein has been shown to improve survival, lower the incidence of poorly differentiated PC, and reduce expression of osteopontin in the prostate of transgenic mice with PC [7]. Cucurbitacins in *Fructus trichosanthis* inhibit growth of various cancer cell lines [8] and of lung xenografts in nude mice [9]. The antioxidants resveratrol and yuccaol in *Y. schidigera* inhibit sarcoma cell proliferation *in vitro* [10]. Here we sought to assess the effects of MINA-05 on the growth of human PC cell lines *in vitro* and against PC-3 cells implanted in the prostate in nude mice.

Materials and Methods

Chemicals and Reagents

MINA-05 (CK Life Sciences Int'l Inc Hong Kong), stored sealed with desiccant at room temperature (RT), was dissolved in DMSO to a final concentration of 0.5% for treatment. To ensure consistency of MINA-05 components between

batches, HPLC profiling and liquid chromatography–mass spectrometry (LC-MS) analysis based on markers selected from the Chinese Pharmacopeia were performed.

LC separations were performed in a Waters (Milford, MA) ACQUITY UPLCTM system using a 50 × 2.1-mm ACQUITY BEH C18 1.7-μm column and a sample volume of 5 μl. The mobile phase was composed of solvent A (0.1% formic acid) and solvent B (acetonitrile) at a constant flow of 0.5 ml/min. The gradient was programmed to increase the amount of solvent B from an initial 40% to 95% in 3 minutes. The composition was held at 100% B for a further 1 minute (3.1–4 minutes) before being returned to the initial condition until 6 minutes. Gomisin A was selected as one of the markers. MS was performed on a Micromass Quattro Premier LC/MS/MS system fitted with an ESI+ interface and controlled by MassLynx software (version 4.0) (Waters). For the MRM transition mode, m/z 399.3 and 330.2 were selected as precursor and product ions, respectively. Cone voltage and collision energy were optimized at 30 and 20 V, respectively. The marker Gomisin A was present at 29 mg/g in MINA-05 ± 10%.

HPLC analysis was performed using a Waters HPLC System (2796XC Bioseparations module) equipped with a Waters 2996 PDA detector with MassLynx NT 4.0 software for data acquisition and processing. HPLC separations of samples were achieved with a Waters Xterra RP18 column (3.9 × 150 mm, particle size of 5 μm) eluted at 1 ml/min with a gradient elution of 5% to 95% acetonitrile in water for 18 minutes.

Cell Lines and Culture

PC-3 (from bone metastasis, p53 null [11]), LNCaP-FGC (lymph node metastasis, p53 wild type [11]), and PZ-HPV-7 (p53 wild type with silent mutation at codon 113 [12]) were obtained from the American Type Culture Collection (ATCC, Rockville, MD). DuCaP and LNCaP-C4-2B were the generous gift of Professor Kenneth Pienta (University of Michigan, Ann Arbor, MI) and LAPC-4 of Professor Charles Sawyers (Memorial Sloan-Kettering Cancer Center, NY). PC-3 and LNCaP-FGC were maintained in RPMI 1640 medium containing 10% FBS. PZ-HPV-7 was maintained in keratinocyte serum-free medium supplemented with bovine pituitary extract (0.05 mg/ml) and epidermal growth factor (0.005 μg/ml). DuCaP (from dura mater metastasis [13], p53 mutation A248W [14]) were cultured in Dulbecco's modified Eagle's medium with 10% FBS and LNCaP-C4-2B in T medium [15]. LAPC-4 (from lymph node [16], p53 mutation, A175H P72R [14]) was maintained in Iscove's modified Dulbecco's medium supplemented with 10% FBS and 10 nmol/l dihydrotestosterone (Sigma Aldrich, Castle Hill, NSW, Australia). All culture media and supplements were obtained from Invitrogen (Melbourne, VIC, Australia) unless indicated otherwise. Cells were maintained under standard culture conditions.

WST-1 Assay

Cells were plated in triplicate in 96-well plates, left 48 hours, then treated with 0.244 to 200 μg/ml MINA-05, 0.5% DMSO vehicle, or medium alone. Cells were seeded at the following concentrations (cells/well): PC-3 (4000),

LNCaP-FGC (1000), LAPC-4 (6000), DuCaP (7500), LNCaP-C4-2B (7500) and PZ-HPV-7 (2000). After 72 hours, viability was assessed by WST-1 assay, which quantifies mitochondrial metabolic activity, as per the manufacturer's instructions (Takara, Madison, WI).

Cell Proliferation Assay

PC-3 ($2.5 × 10^5$ cells) and LNCaP-FGC ($1.5 × 10^5$ cells) were plated in 150 cm^2 flasks for 48 hours then treated with a $2 × IC_{50}$ dose of MINA-05 or 0.5% DMSO vehicle. After 15 minutes, 1, 4, 16, 24, and 48 hours, cells were harvested by trypsinization with pooling of adherent and nonadherent cells. Cells were washed twice in phosphate-buffered saline (PBS) and viability was assessed with trypan blue. Cell pellets were lysed in M-PER buffer (Pierce, Rockford, IL), snap-frozen in liquid nitrogen, and stored at −20°C until analyzed by Western blot.

Clonogenic Survival

Cells were pretreated with $^1/_2$ ×, 1 ×, and $2 × IC_{50}$ doses of MINA-05 or 0.5% DMSO vehicle for 72 hours in 25 cm^2 flasks. Cells were harvested and viability was determined with trypan blue. For clonogenic assays on plastic (anchorage dependent), 250 viable cells per well were seeded in six-well plates, then incubated without treatment for 7 (LNCaP-FGC) or 9 days (PC-3), based on known doubling times. Media were refreshed every 3 days. Cells were then stained with 0.5% crystal violet/20% methanol and colonies of >50 cells were counted by inverted light microscopy. For soft agar assays (anchorage independent), cells were harvested after treatment, and $5 × 10^4$ cells in medium were mixed 1:1 with 0.6% agar (0.3% agar) before seeding into six-well plates precoated with 1.2% agar mixed 1:1 with medium (0.6% agar). The plates were incubated for 14 days and colonies of >50 cells in 10 random fields were counted per well by inverse light microscopy.

Cell Cycle Analysis

PC-3 ($2.5 × 10^5$) and LNCaP-FGC ($1.5 × 10^5$) cells per 150 cm^2 flask were left 48 hours before treatment with MINA-05 at $^1/_2$ ×, 1 ×, and $2 × IC_{50}$ or 0.5% DMSO vehicle for 72 hours (<75% confluent). Adherent cells (collected by trypsinization) were pooled with nonadherent cells and viability was determined with trypan blue. Cells were washed twice with PBS, fixed in ice-cold 70% ethanol, and stored at 4°C until use. Cells ($5 × 10^5$) were treated with 50 μg/ml RNase A (Sigma), stained in 1.167 μg/ml propidium iodide (Sigma) for 30 minutes at 4°C in the dark, then analyzed on a FACSCanto flow cytometer (Becton Dickinson, Bedford, MA) to analyze DNA content; $5 × 10^4$ events were collected. Cell cycle distribution was analyzed with FACSDiva software.

Immunohistochemistry

For activated caspase-3 staining, PC-3 and LNCaP-FGC cells were grown on chamber slides at $(1 \text{ to } 2) × 10^3$ cells per well for 48 hours, then treated with MINA-05 at $^1/_2$ ×, 1 ×, and $2 × IC_{50}$ or 0.5% DMSO vehicle for 72 hours before fixation in ice-cold acetone. Positive control cells were treated with

1 μg/ml cisplatin to induce apoptosis. Cleaved caspase-3 was detected using rabbit monoclonal antibody (5A1; Cell Signaling Technology, Danvers, MA) then biotinylated goat anti-rabbit IgG antibody (Vector Laboratories, Burlingame, CA), and color was developed using a VECTASTAIN ABC kit (Vector Laboratories) and DAB chromogen (Dako, Carpinteria, CA). Over 200 nuclei were counted per well and cells were scored for activated caspase-3 staining.

For pancytokeratin staining, frozen, acetone-fixed 5-μm sections of lymph nodes embedded in Tissue-Tek ornithine carbamoyltransferase (OCT) compound (Sakura Finetechnical, Koto-ku, Tokyo, Japan) on Superfrost Ultra Plus slides (Menzel-Glaser, Raunschweig, Germany) were air-dried, rinsed in PBS, quenched for endogenous peroxidase, and blocked for nonspecific protein binding before being stained with pancytokeratin antibody 1:5000 (Z0622; Dako) for 1 hour, and antirabbit antibody 1:100 (Vector Laboratories). Color was developed using 1:100 HRP-conjugated avidin–biotin complex (Vector Laboratories) then 1:50 DAB (Dako) before counterstaining with Harris hematoxylin.

Western Blotting

Protein concentrations of cleared whole-cell lysates were measured using BCA Protein Reagent Kit (Pierce). Proteins were analyzed in equally loaded samples by Western blot, using a rabbit polyclonal antibody to cdc2 phosphorylated at Tyr15 (p-cdc2) (9111; Cell Signaling Technology; 1:1000), a mouse monoclonal cdc2 antibody (sc-54; 1:200), a mouse monoclonal antibody to cyclin B1 (sc-254; 1:200), and a rabbit polyclonal antibody to cdc25C (sc-327; 1:400) (all from Santa Cruz Biotechnology, Santa Cruz, CA) and a mouse monoclonal antibody against human β-actin (AC-15, 1:7500; Sigma). Briefly, samples were run on 10% sodium dodecyl sulfate (SDS)–polyacrylamide gels and electrophoretically transferred (SDS–PAGE) to nitrocellulose membranes (Bio-Rad Laboratories, Hercules, CA). Nonspecific binding sites were blocked with 5% skim milk powder diluted in PBS with 0.1% Tween 20 (SMP/PBST). Membranes were hybridized with primary antibody followed by horseradish peroxidase–linked goat anti-rabbit and goat anti-mouse secondary antibodies (Santa Cruz) also diluted in SMP/PBST. Proteins were visualized by enhanced chemiluminescence (Pierce). Each blot was stripped with Restore Western blot stripping buffer (Pierce) for reprobing with other antibodies.

Orthotopic PC-3 Tumor Xenograft Study

Permission for this study was obtained from the Animal Ethics Committee, University of New South Wales (UNSW), in line with the National Institutes of Health *Guide for the Care and Use of Laboratory Animals*. Sixty 6- to 7-week-old male BALB/c *nu/nu* (nude) mice from the Biological Resources Centre, UNSW, were housed at four to five per cage under specific pathogen-free conditions. Mice were anesthetized with isoflurane (Abbott Laboratories, Botany, NSW, Australia) and placed in a supine position, and the prostate was exposed by laparotomy. PC-3 cells were orthotopically implanted at 10^6 cells in 40 μl PBS (30 mice per day) before closing and stitching the wound. Mice were randomized into

four experimental groups (n = 15). Daily gavage (ball-tipped 18-gauge needle) was started 3 days after tumor injection at 2, 1, 0.5, or 0 mg MINA-05 in 400 μl 1% carboxymethyl cellulose/2.5% DMSO daily. On day 21, five mice per group were sacrificed and the remainder after 42 days. Prostates were weighed and volumes were assessed by the formula $V = \pi/6(d_1 d_2)^{3/2}$, where d_1 and d_2 are diameters at right angles. The draining, caudal, and renal lymph nodes were frozen in Tissue-Tek OCT compound (Sakura Finetechnical), sectioned at 5 μm, and stained with hematoxylin and eosin or antipancytokeratin antibody. Lymph nodes were scored for intensity (1+, weak; 2+, moderate; 3+, strong) and pattern (percent) of distribution of cytokeratin-positive PC-3 tumor cell infiltration.

Statistical Analysis

GraphPad PRISM (GraphPad Software, San Diego, CA) was used for statistical analysis. Data are expressed as mean ± SD. In dose–response experiments, treatments were compared by one-way analysis of variance then Tukey's post-tests. In time course experiments, two-tailed t tests were used; $P < .05$ was considered significant. For lymph node invasion, analysis of variance was used followed by Dunnett's multiple comparison test. For activated caspase-3 expression, Kruskal–Wallis test and Bonferroni post hoc tests were used. To have an optimal sample size, the data from three experiments were analyzed together.
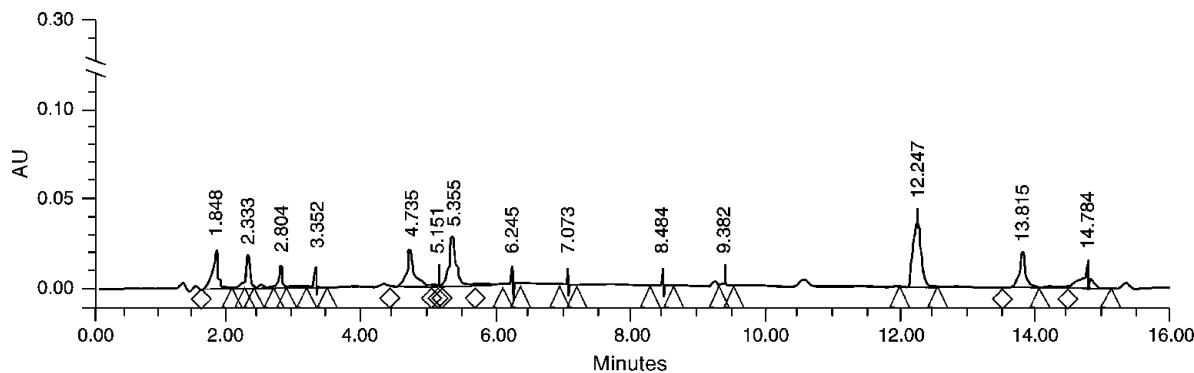
Results

MINA-05

Batch-to-batch reproducibility was assessed by comparing peak retention times of the major components and ascertaining that they were within a window of 2% variation in retention in keeping with standard assessment techniques of the laboratory. A representative chromatogram showing reverse phase HPLC separation of MINA-05 is shown in Figure 1.

Growth Inhibition by MINA-05 of Human PC Cells

After 72 hours of MINA-05 treatment, mitochondrial metabolic activities were significantly and dose-dependently decreased in all PC cell lines tested and in nontumorigenic PZ-HPV-7 cells (Figure 2*A*). The IC$_{50}$ values (μg/ml) were 13.39 (LNCaP-C4-2B), 46.34 (PC-3), and 1.21 (PZ-HPV-7) for HRPC cell lines, and 25.11 (LNCaP-FGC), 35.53 (DuCaP), and 4.24 (LAPC-4) for androgen-sensitive lines. Sensitivity to MINA-05 did not correlate with androgen responsiveness, site of isolation of the tumor cell line, or p53 status.

Treatment with 2 $\times$ IC$_{50}$ MINA-05 inhibited proliferation of LNCaP-FGC and PC-3 cells (Figure 2, *B* and *C*). Both showed no significant change in cell number over 48 hours of MINA-05 treatment, whereas vehicle-treated cells, used as controls in all experiments, increased exponentially from 24 hours. There were significantly fewer viable PC-3 and LNCaP-FGC cells in MINA-05–treated flasks relative to controls at 24 ($P < .05$) and 48 hours ($P < .01$).

Figure 1. *Representative chromatogram showing reverse phase HPLC separation of MINA-05. Batch-to-batch reproducibility was assessed by comparing peak retention times of the major components and ascertaining that they were within a window of 2% variation in retention in keeping with standard assessment techniques of the laboratory.*
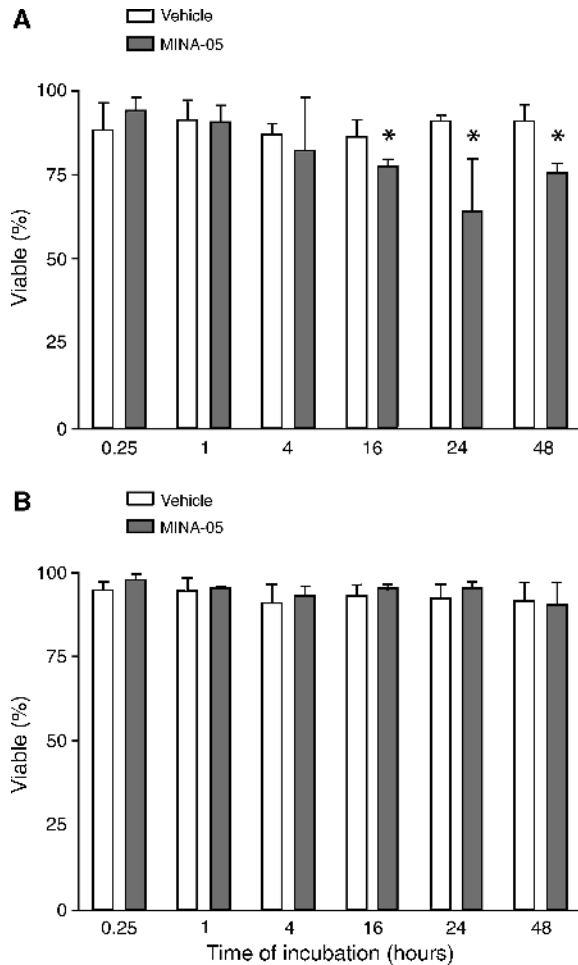
MINA-05 Treatment

MINA-05 treatment at $2 \times IC_{50}$ induced a modest, significant decrease in the proportion of viable LNCaP-FGC cells relative to controls after 16 to 48 hours ($P < .05$; Figure 3*A*), but not in PC-3 cells (Figure 3*B*). Morphological changes were seen after MINA-05 treatment in both LNCaP-FGC and PC-3 cells (not shown), with flattening, cell enlargement, and increased plastic adherence after 1 hour at lower MINA-05
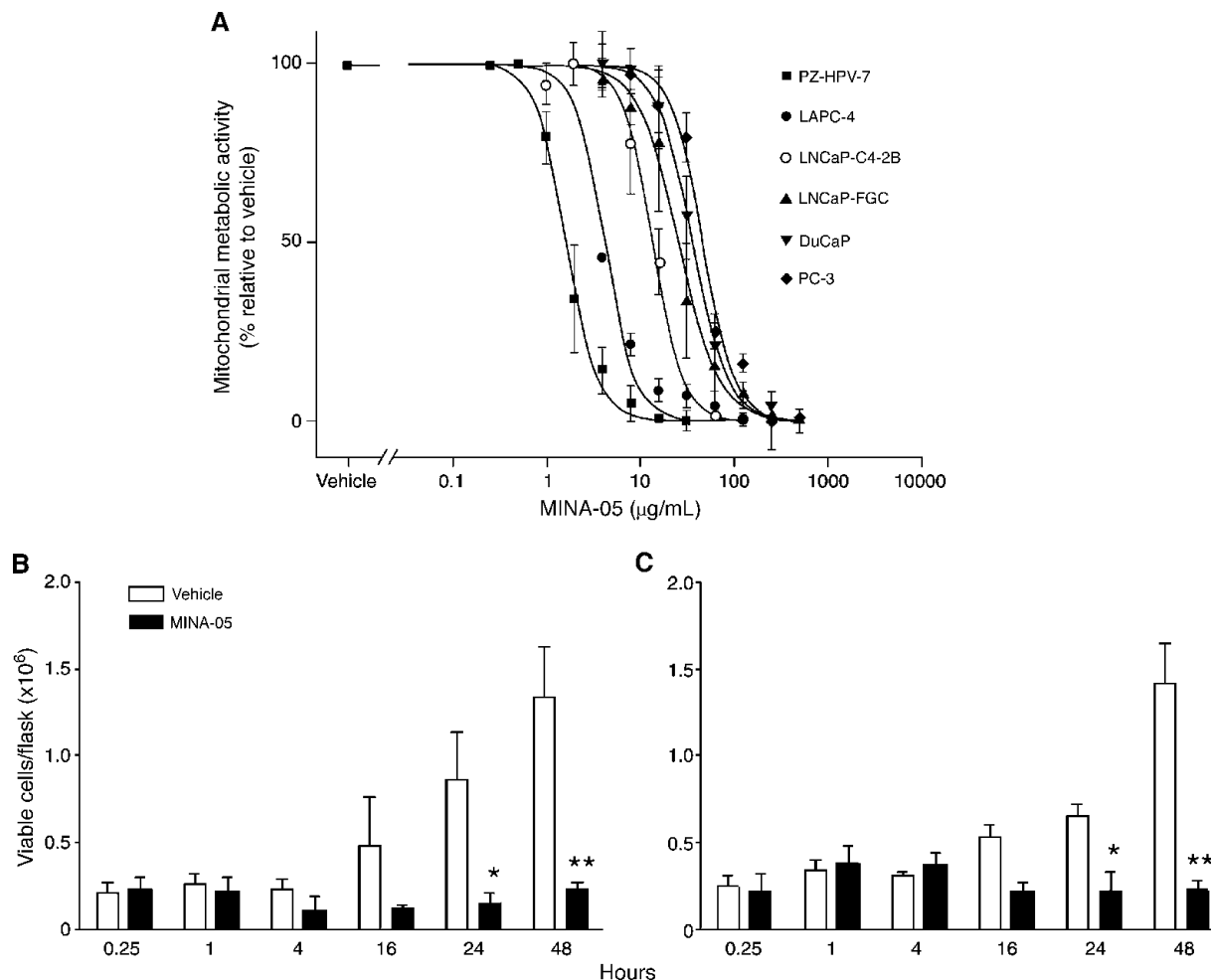
Figure 2. *Effect of MINA-05 treatment on proliferation of PC cell lines* in vitro. *(A) Cells seeded in 96-well plates were treated with 0.24 to 500 μg/ml MINA-05 or 0.5% DMSO (vehicle). After 72 hours, effects on cell proliferation were determined by WST-1 assay. Additional wells assayed without treatment confirmed that the DMSO vehicle did not affect cell viability (not shown). (B) LNCaP-FGC and (C) PC-3 cells were treated in 150 cm² flasks with $2 \times IC_{50}$ MINA-05 or vehicle. After the indicated time (hours) cells were harvested and cell viability was assessed by trypan blue exclusion. Data indicate mean ± SD (n = 3). *P < .05, **P < .01 relative to vehicle.*

Figure 3. *Effects of MINA-05 treatment on viability of PC cells* in vitro. *(A) LNCaP-FGC and (B) PC-3 cells were treated with $2 \times IC_{50}$ dose of MINA-05 or 0.5% DMSO (vehicle, V) for the time indicated (hours). Adherent and non-adherent cells were pooled, and viability was determined by using trypan blue. Graphs indicate mean ± SD of three independent experiments. *P < .05, relative to vehicle.*

doses. At $2 \times IC_{50}$, LNCaP-FGC cells became smaller and rounded, whereas PC-3 cells appeared more dendritic.

MINA-05 Pretreatment Inhibited Colony Formation

Pretreatment of LNCaP-FGC cells with IC_{50} and $2 \times IC_{50}$ doses of MINA-05, but not at $\frac{1}{2} \times IC_{50}$, significantly suppressed colony formation in soft agar relative to vehicle-treated wells (37 ± 2 colonies per 10 fields of view) with 0 ± 0 (P < .001), 0 ± 0 (P < .001), and 1 ± 1 (P < .001), respectively (Figure 4A). MINA-05 pretreatment also resulted in abrogation of colony formation on hard plastic from 310 ± 12 colonies per well (vehicle-treated cells; Figure 4B) to 1 ± 1 (P < .001), 3 ± 1 (P < .001), and 8 ± 2 (P < .001), respectively.

Pretreatment of PC-3 cells with IC_{50} and $2 \times IC_{50}$ doses of MINA-05 elicited a dose-dependent decrease in colony numbers, whereas treatment at $\frac{1}{2} \times IC_{50}$ did not significantly alter clonogenicity relative to controls. Pretreatment with MINA-05 at IC_{50} and $2 \times IC_{50}$ doses of MINA-05 decreased colony numbers in soft agar from control numbers of 77 ± 6 colonies per 10 fields of view (Figure 4C) to 38 ± 12 (P < .05) and 3.4 ± 1 (P < .001), and on hard plastic from 150 ±

25 to 41 ± 14 and 4 ± 1 colonies per well, respectively (both P < .01; Figure 4C). MINA-05−resistant PC-3 colonies (in agar) appeared larger than those in vehicle-treated cultures (Figure 4A).

MINA-05 Induced Cell Cycle Arrest at the G_2M Phase

Cell cycle distribution of LNCaP-FGC and PC-3 cells was analyzed 72 hours after treatment with MINA-05 at $\frac{1}{2} \times IC_{50}$, IC_{50}, and $2 \times IC_{50}$ (Figure 5). G_2M arrest was seen after MINA-05 treatment at all doses in both cell lines, with changes in the proportion of S-phase cells in LNCaP-FGC but not PC-3 cells compared with control cells. LNCaP-FGC cells accumulated in S phase after treatment at $\frac{1}{2} \times IC_{50}$ dose, but showed a decrease in the S-phase population at IC_{50}-MINA-05.

### Apoptosis Was Increased in LNCaP-FGC but Not PC-3 Cells by MINA-05 Treatment

Apoptosis, as seen by the presence of a modest sub-G_1 peak by flow cytometry, was induced in LNCaP-FGC cells treated for 72 hours at IC_{50} and $2 \times IC_{50}$ doses of MINA-05 but not at $\frac{1}{2} \times IC_{50}$ (Figure 5A). This was confirmed by an increase in activated caspase-3−positive cells counted per 10 fields (±SD from $n = 6$) from 0.76 ± 1.07 in vehicle-treated cells to 6.52 ± 5.59 [P = .051 and 7.45 ± 4.05 (P = .017) in IC_{50} and $2 \times IC_{50}$ MINA-05 treated cells, respectively), but not in those treated at $\frac{1}{2} \times IC_{50}$ (0.49 ± 0.18, P = 1.00). There was no sub-G_1 peak in PC-3 cells (Figure 5B) nor an increase in activated caspase-3−positive cells from vehicle-treated (1.69 ± 0.06) to MINA-05−treated cells at any dose (range, 1.24 ± 0.67 to 1.97 ± 2.26).

### Western Blotting Analysis of G_2M Regulatory Proteins

To investigate the mechanisms involved in G_2M cell accumulation after MINA-05 exposure, Western blotting analysis for changes in the levels of key cell cycle factors was undertaken. Cdc2 kinase assembly involves binding to cyclin B1 and phosphorylation at Thr14 (phosphorylated through Myt1) and Tyr15 (phosphorylated by Wee1) [17]. Mitosis is induced when cdc2−cyclin B1 complex accumulates in the nucleus and is activated by dephosphorylation of Thr14 and Tyr15 by cdc25 [17,18]. In this study, cyclin B1 expression was decreased by MINA-05 treatment after 1 hour in LNCaP-FGC (Figure 6A) and after 4 hours in PC-3 (Figure 6B) cells. G_2M transition requires cdc25C to dephosphorylate cdc2 [18]. Here, levels of cdc2 decreased after 48 hours of treatment in PC-3 cells; p-cdc2 expression remained unchanged. Treatment of LNCaP-FGC cells induced a transient decrease in cdc2 at 1 hour, with sustained decrease from 16 to 48 hours. The ratio of p-cdc2 to cdc2 protein levels was increased in LNCaP-FGC cells at 1, 16, 24, and 48 hours after treatment, indicating that cdc2 remained inactive. Cdc25C is detectable as three forms: unphosphorylated cdc25C (fastest migratory form), phosphorylated on Ser16 (intermediate band), and the hyperphosphorylated (active) form (slowest migrating band) present during mitosis [19]. No unphosphorylated cdc25C

was detected in either vehicle- or MINA-05–treated LNCaP-FGC cells. The phosphorylated form becomes undetectable after 1-hour MINA-05 treatment, and both the phosphorylated and the active forms are undetectable from 4 hours

treatment onward (Figure 6A). In contrast, unphosphorylated cdc25C is present in PC-3 cells but becomes undetectable after 1-hour MINA-05 treatment. From 16 hours onward, all forms of cdc25C disappear with MINA-05 treatment
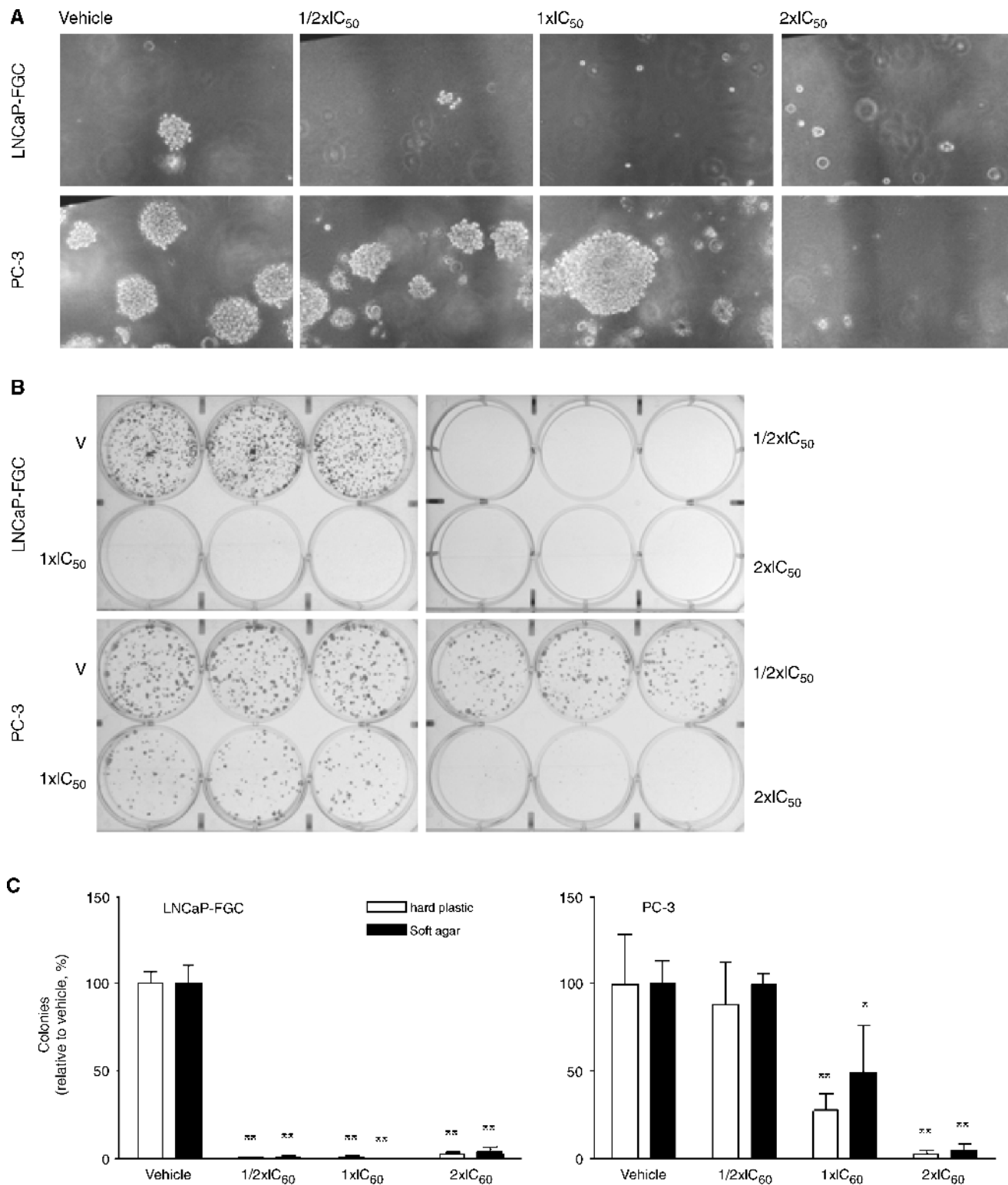
Figure 4. *Effect of MINA-05 pretreatment on colony formation of PC cell lines in vitro. LNCaP-FGC and PC-3 cells were treated with MINA-05 at $^1/_2 \times IC_{50}$, IC_{50}, or $2 \times IC_{50}$ concentrations, or 0.5% DMSO (vehicle), in triplicate. After 72 hours, cells were harvested, cell viability was determined by trypan blue exclusion assay, and viable cells were seeded for clonogenic assays (A) in soft agar and (B) on plastic. (C) Total number of colonies (>50 cells) was counted by using an inverted light microscope (original magnification, $\times 38.4$). Graphs indicate mean ± SD of three independent experiments. *P < .05, **P < .01 relative to vehicle.*
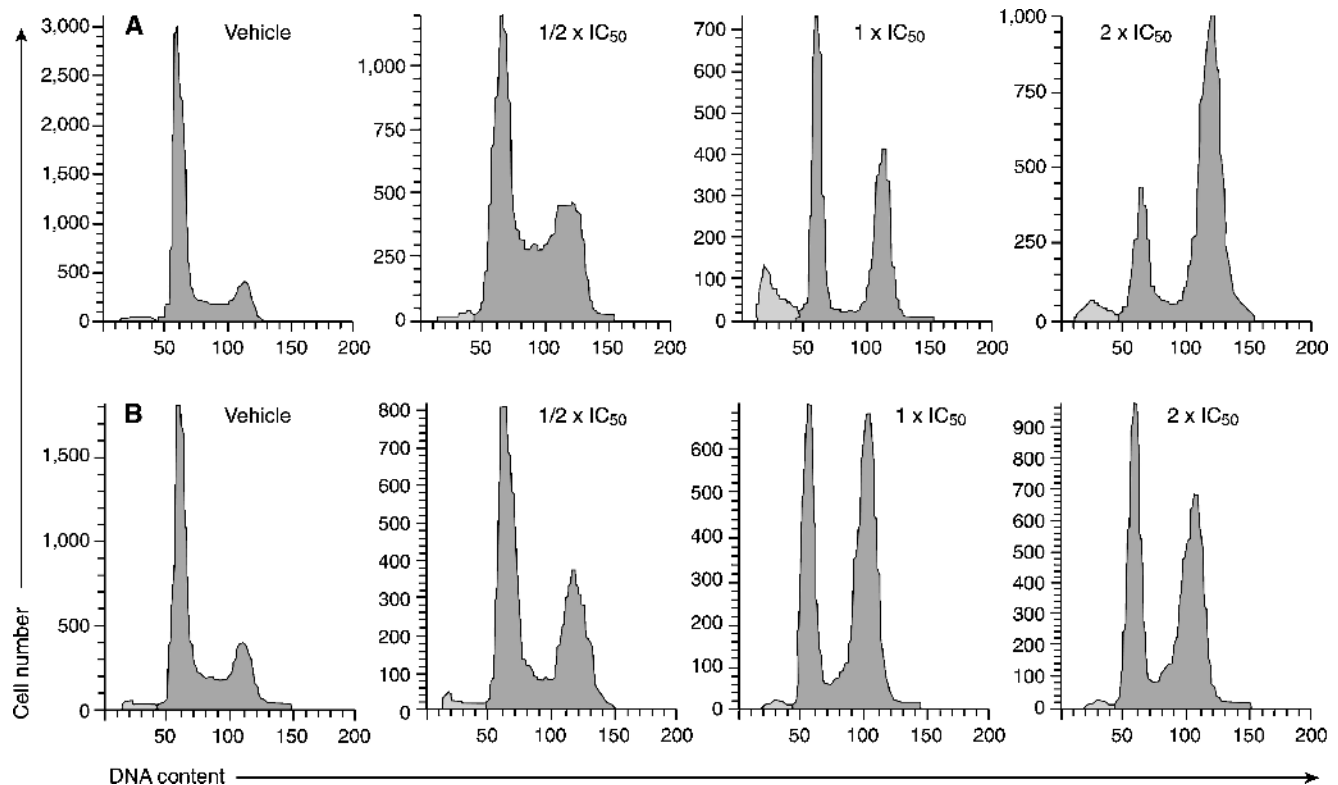
Figure 5. *MINA-05 treatment increases G_2M population in PC cells* in vitro. *(A) LNCaP-FGC and (B) PC-3 cells were treated with $^1/_2 \times IC_{50}$, IC_{50}, or $2 \times IC_{50}$ doses of MINA-05 or 0.5% DMSO (vehicle, V) for 72 hours as shown. Adherent and nonadherent cells were harvested, stained with propidium iodide, and analyzed using FACSCanto. Representative results from three independent experiments are shown.*

(Figure 6*B*). The decrease in cdc25C levels was not associated with an increase in p-cdc2 levels in PC-3 cells, which may indicate that levels of the cdc2 kinases Myt1 and Wee1, which maintain phosphorylation at Tyr15 and Thr14, respectively, on cdc2, are also altered by MINA-05 treatment. This was not assessed in this study.

Treatment with MINA-05 Inhibited Lymph Node Invasion by PC-3 Cells In Vivo

Starting 3 days after intraprostatic injection of PC-3 cells, treatment by gavage with MINA-05 at 0.5, 1, or 2 mg/d or vehicle was performed daily for 39 days. There were six unrelated deaths. Mice were sacrificed at 21 or 42 days postimplantation to examine the effects of treatment. At 21 days, prostate tumor weights (mean, 60.3 mg; range, 32.3–86.5 mg) and volumes (mean, 69.5 mm^3; range, 32.3–86.5 mm^3) varied, but showed no significant differences between treatment groups. After 42 days, tumors, present in 34 of 34 mice, were slightly smaller after MINA-05 treatment (0.5 mg/d: 112 mg [76–151]; 1 mg/d: 100 mg [46–144]; 2 mg/d: 119 mg [80–163]) compared with vehicle (126 mg [84–159]) but with no significant differences between groups. Enlargement of intraperitoneal lymph nodes occurred in six of nine vehicle-treated mice, seven of nine, six of eight, and eight of eight mice treated with 0.5, 1 mg/ml, and 2 mg/d MINA-05, respectively. There was no significant difference in the size of the enlarged lymph nodes in the different treatment groups. The pattern of PC-3 cell invasion assessed by pancytokeratin staining within lymph nodes

was diffuse (Figure 7, *A–C*) or peripheral (Figure 7*D*). The percentage of pancytokeratin-positive cells indicated that lymph node invasion was decreased in mice on higher MINA-05 doses (1–2 mg/d) compared with vehicle treatment. From examining 21 to 24 lymph nodes per group, mean percentage invasion was reduced from 44.2% in control mice (range, 20–90%) and 53.7% (range, 20–90%) ($P > .05$) in mice given 0.5 mg/d to 34.3% (range, 10–60%) ($P < .05$) and 30.5% (range, 0–50%) ($P < .01$) in mice given 1 and 2 mg/d, respectively (Figure 7*E*).

Discussion

MINA-05 was shown to inhibit cell proliferation in human androgen-sensitive and HRPC cell lines, as well as in immortalized normal prostate cells. Sensitivity to MINA-05 did not correlate with p53 status, androgen responsiveness, or the metastatic site from which the cell line came. This effect was associated with cell cycle arrest in G_2M and an increase in apoptosis at high doses in LNCaP-FGC but not in PC-3 cells.

Abrogation of colony formation (Figure 4) occurred in LNCaP-FGC cells at doses inducing ~10% decrease in cell number by WST-1 assay (Figure 2). The data suggest that MINA-05 may slow cell proliferation with the surviving population of LNCaP-FGC cells entering irreversible cell cycle arrest or commitment to a cell death pathway. The presence of a sub-G_1 population of LNCaP-FGC cells and cleaved caspase-3 staining suggests induction of apoptosis

by MINA-05 at higher doses. As this did not occur in PC-3 cells, MINA-05 may inhibit PC-3 cell growth through a mechanism other than apoptosis.

G$_2$M arrest occurred after MINA-05 treatment in both LNCaP-FGC and PC-3 cell lines. We used Western blotting for expression of key regulators of G$_2$M transition to determine the mechanism. Activation of nuclear cdc2/cyclin B1 complex by dephosphorylation of cdc2 at Thr14 and Tyr15 by cdc25C is required for entry into mitosis [17]. DNA damage through irradiation or treatment with drugs such as etoposide interferes with cdc2 dephosphorylation by cdc25C phosphatase [20]. Loss (LNCaP-FGC) or decrease (PC-3 cells) of cdc25C 1 hour after treatment with MINA-05 indicates that it might cause DNA damage, with kinetics like those seen with etoposide on CHO cells [21]. Inactivation of cdc25C can involve phosphorylation through protein kinases Chk-1 and -2 [17]. DNA damage may also turn on phosphorylation of Tyr15 on cdc2 by Mik1 [22]. These mechanisms were not investigated further in this study.

Cyclin B1 is ubiquitinated and degraded late in mitosis [23,24]. We have shown that MINA-05 treatment decreased cyclin B1 protein to undetectable levels in both LNCaP-FGC and PC-3 cells (Figure 6). Levels of phosphorylated (inactive) cdc2 were not substantially changed by treatment of PC-3 cells before 24 hours. Levels of p-cdc2, compared with total cdc2 levels, were markedly increased in treated LNCaP-FGC cells relative to vehicle controls; this was associated with decreased cdc2 phosphatase, cdc25C. This suggests that MINA-05 induces cell cycle arrest primarily by decreasing cdc2/cyclin B1 activity through decreasing cyclin B1 levels and, in LNCaP-FGC cells by decreasing total cdc2 levels and increasing inactive p-cdc2. Alternatively, MINA-05–induced cell cycle arrest may occur late in mitosis, when cyclin B1 levels are decreased. Arrest in M phase by antitubulin agents such as paclitaxel involves activation of cdc2 and an increase in cyclin B1 levels [25], effects that were not seen here. This suggests that MINA-05 is not causing mitotic arrest via effects on microtubules.
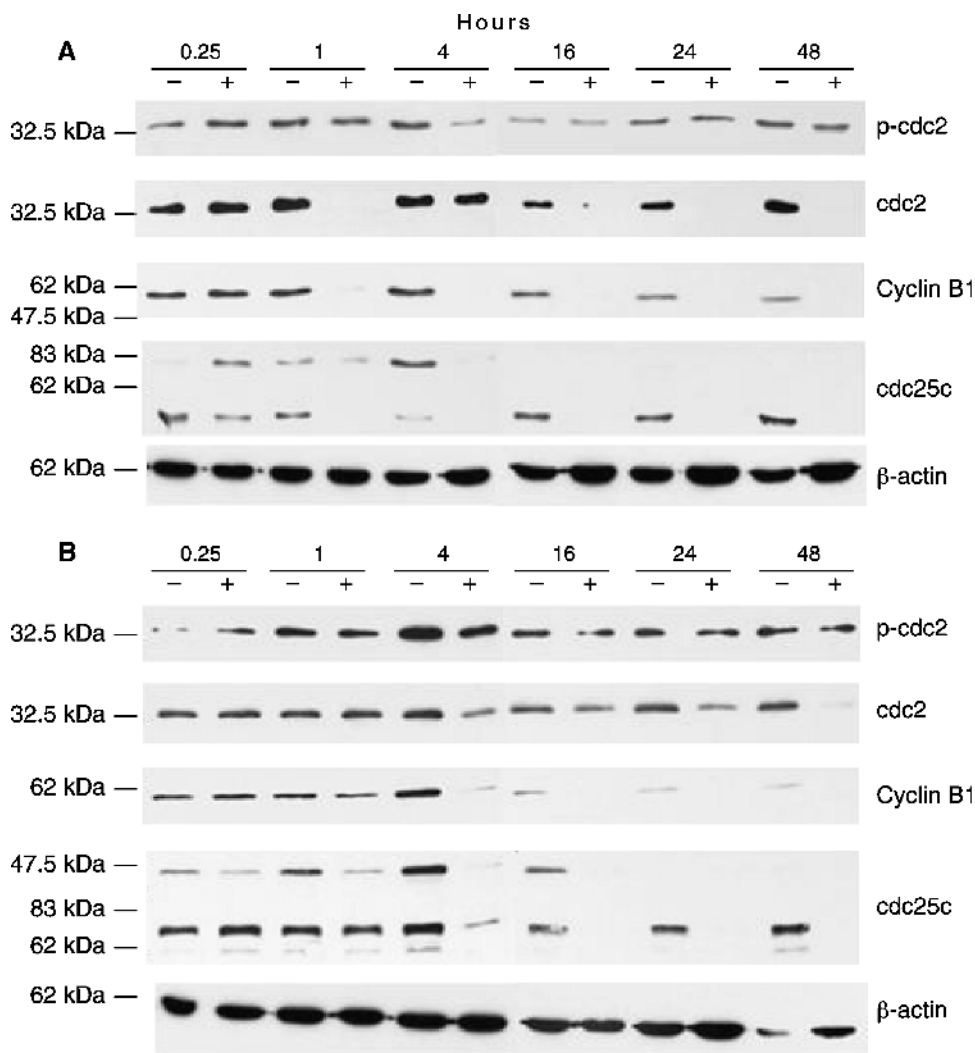
Figure 6. *Expression of cell cycle–regulatory proteins after MINA-05 treatment. (A) LNCaP-FGC and (B) PC-3 cells were treated with 2 × IC$_{50}$ MINA-05 or vehicle for the time indicated (hours), and the adherent and nonadherent cells were collected and lysed. Total protein (60 μg) was subjected to SDS-PAGE and Western blotting analysis by using antibodies against p-cdc2, cdc2, cyclin B1, and cdc25C. Representative results are shown.*
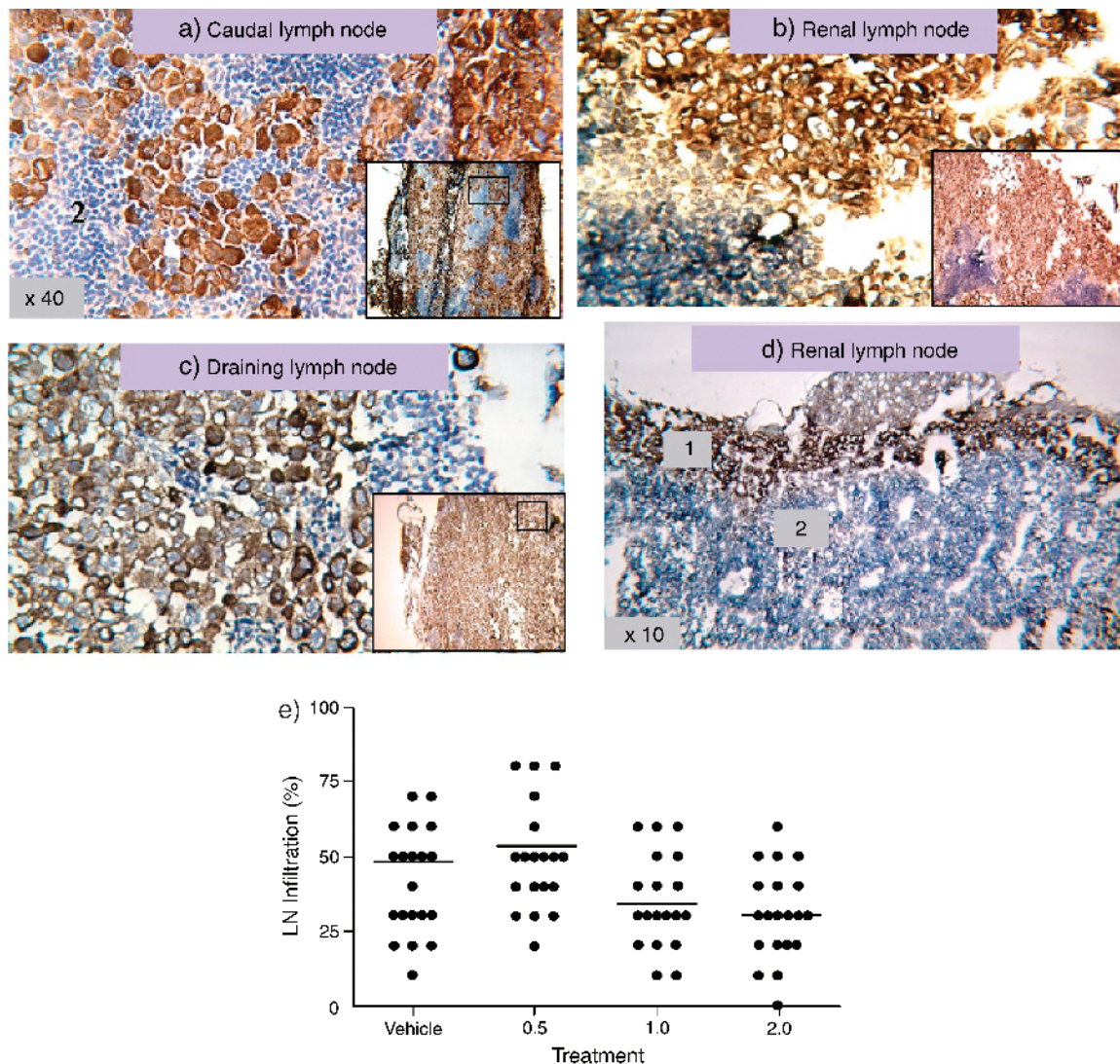
Figure 7. *PC-3 cell invasion of local lymph nodes after orthotopic implantation in nude mice. Photomicrographs showing pancytokeratin-positive PC-3 tumor cells (brown) invading local lymph nodes (LN) after intraprostatic injection in nude mice. (A, B, C) Diffuse invasion in vehicle-treated mouse (original magnification, ×40). Insets show low-power staining and area selected at higher power. (D) Peripheral LN invasion in mouse treated with 2 mg/day MINA-05 (original magnification, ×10). 1, Positive cytokeratin PC-3 tumor cell metastasis in lymph node. 2, Lymphocytes in paracortical area. (E) Graph showing percent infiltration of LN in vehicle- or MINA-05–treated mice bearing orthotopic PC-3 tumors. Bars represent mean values.*

G_2M arrest in p53 null cells tends to be transient [26]. Human colorectal cancer HCT116 cells, in which p53 had been inactivated by homologous recombination, entered temporary G_2M arrest after ionizing radiation, whereas isogenic cells with functional p53 showed prolonged G_2M arrest [27]. After the p53-null cells escaped arrest, the proportion of cells in mitosis was higher than in untreated cells [25]. This may explain our observation in PC-3 cells, which are p53 null [11], where pretreatment with IC_{50} MINA-05 resulted in formation in agar of colonies larger than after pretreatment with vehicle alone. G_2M arrest in PC-3 cells after MINA-05 treatment was not accompanied by a decrease in S-phase cells compared with controls, suggesting that PC-3 cells are not completely arrested after treatment (Figure 5). Inhibition of cdc2 is one of the means by which p53 blocks entry at the G2 checkpoint [26]. Levels of cdc2 were only margin-

ally decreased after 48 hours of treatment of PC-3, compared with rapid effects in LNCaP-FGC cells that express phenotypically wild-type p53 (Figure 5). PC-3 cells treated at lower concentrations of MINA-05 may escape G_2M arrest and proliferate to form colonies, whereas treatment may induce irreversible arrest in wild-type p53 LNCaP-FGC cells, preventing colony formation (Figure 4).

Despite the finding that PC-3 cells were less sensitive to growth inhibition by MINA-05 than by LNCaP-FGC, there was an interesting response *in vivo* after orthotopic implantation. PC-3 cells were selected for these studies as they spontaneously spread to local lymph nodes. Whereas MINA-05 treatment did not inhibit primary tumor growth, there was significant inhibition of the extent of tumor invasion into local lymph nodes by higher doses (1–2 mg/d) of MINA-05. Because the mice were immunodeficient, this

reflects a direct effect on the tumor cells, rather than being an immune-mediated effect. The data suggest that higher doses of MINA-05 may inhibit lymph node metastases.

Cells in G_2M are more radiosensitive than cells in other phases of the cell cycle [28]. Transient induction of G_2M arrest thus has the potential to increase sensitivity to radiotherapy, suggesting that MINA-05 has a potential role as a radiosensitizer. Overall, the data indicate that MINA-05 treatment has advantages for patients with PC, and further investigation to determine potential synergy with other agents, such as radiotherapy, is warranted.

References

[1] Jemal A, Murray T, Ward E, Samuels A, Tiwari RC, Ghafoor A, Feuer EJ, and Thun MJ (2005). Cancer statistics, 2005. *CA Cancer J Clin* **55**, 10–30.

[2] Engel LW and Straus SE (2002). Development of therapeutics: opportunities within complementary and alternative medicine. *Nat Rev Drug Discov* **1**, 229–237.

[3] Talalay P and Talalay P (2001). The importance of using scientific principles in the development of medicinal agents from plants. *Acad Med* **76**, 238–247.

[4] Hsieh TC, Lu X, Guo J, Xiong W, Kunicki J, Darzynkiewicz Z, and Wu JM (2002). Effects of herbal preparation Equiguard on hormone-responsive and hormone-refractory prostate carcinoma cells: mechanistic studies. *Int J Oncol* **20**, 681–689.

[5] Wang HZ, Zhang Y, Xie LP, Yu XY, and Zhang RQ (2002). Effects of genistein and daidzein on the cell growth, cell cycle, and differentiation of human and murine melanoma cells. *J Nutr Biochem* **13**, 421–426.

[6] Chen WF, Huang MH, Tzang CH, Yang M, and Wong MS (2003). Inhibitory actions of genistein in human breast cancer (MCF-7) cells. *Biochim Biophys Acta* **1638**, 187–196.

[7] Mentor-Marcel R, Lamartiniere CA, Eltoum IA, Greenberg NM, and Elgavish A (2005). Dietary genistein improves survival and reduces expression of osteopontin in the prostate of transgenic mice with prostatic adenocarcinoma (TRAMP). *J Nutr* **135**, 989–995.

[8] Jayaprakasam B, Seeram NP, and Nair MG (2003). Anticancer and antiinflammatory activities of cucurbitacins from *Cucurbita andreana*. *Cancer Lett* **189**, 11–16.

[9] Sun J, Blaskovich MA, Jove R, Livingston SK, Coppola D, and Sebti SM (2005). Cucurbitacin Q: a selective STAT3 activation inhibitor with potent antitumor activity. *Oncogene* **24**, 3236–3245.

[10] Balestrieri C, Felice F, Piacente S, Pizza C, Montoro P, Oleszek W, Visciano V, and Balestrieri ML (2006). Relative effects of phenolic constituents from *Yucca schidigera* Roezl bark on Kaposi's sarcoma cell proliferation, migration, and PAF synthesis. *Biochem Pharmacol* **71**, 1479–1487.

[11] Carroll AG, Voeller HJ, Sugars I, and Gelmann EP (1999). p53 oncogene mutations in three human prostate cancer cell lines. *Prostate* **23**, 123–134.

[12] Jackson P, Grimm M-O, Kingsley EA, Brosius U, Antalis T, Yardley G, and Russell PJ (2002). Relationship between expression of KAI1 metastasis suppressor gene, mRNA levels and p53 in human bladder and prostate cancer cell lines. *Urol Oncol* **7**, 99–104.

[13] Lee Y-G, Kornechuk S, Lehr J, Whitney S, Vessela R, and Pienta KJ (2003). Establishment and characterization of a new human prostatic cancer cell line: DuCaP. *In Vivo* **15**, 157–162.

[14] van Bokhoven A, Varella-Garcia M, Korch C, Johannes WU, Smith EE, Miller HL, Nordeen SK, Miller GJ, and Lucia MS (2003). Molecular characterization of human prostate carcinoma cell lines. *Prostate* **57**, 205–225.

[15] Thalmann GN, Anezinis PE, Chang SM, Zhau HE, Kim EE, Hopwood VL, Pathak S, von Eschenbach AC, and Chung LW (1994). Androgen-independent cancer progression and bone metastasis in the LNCaP model of human prostate cancer. *Cancer Res* **54**, 2577–2581.

[16] Klein KA, Reiter RE, Redula J, Moradi H, Zhu XL, Brothman AR, Lamb DJ, Marcelli M, Belldegrun A, Witte ON, et al. (1997). Progression of metastatic human CaP to androgen independence in immunodeficient SCID mice. *Nat Med* **3**, 402–408.

[17] Stark GR and Taylor WR (2004). Analyzing the G2/M checkpoint. *Methods Mol Biol* **280**, 51–82.

[18] Draetta G and Eckstein J (1997). Cdc25 protein phosphatases in cell proliferation. *Biochim Biophys Acta* **1332**, M53–M63.

[19] Nilsson I and Hoffman I (2000). Cell cycle regulation by the Cdc25 phosphatase family. *Prog Cell Cycle Res* **4**, 107–114.

[20] Peng C-Y, Graves PR, Thoma RS, Wu Z, Shaw AS, and Piwnica-Worms H (1997). Mitotic and G2 checkpoint control: regulation of 14-3-3 protein binding by phosphorylation of Cdc35C on serine-216. *Science* **277**, 1501–1505.

[21] Lock RB and Ross WE (1990). Possible role for p34cdc2 kinase in etoposide-induced cell death of Chinese hamster ovary cells. *Cancer Res* **50**, 3767–3771.

[22] McGowan CH (2002). Checking in on Cds 1 (Chk2): a checkpoint kinase and tumor suppressor. *Bioessays* **24**, 502–511.

[23] Smits VA, Klompmaker R, Arnaud L, Fijksen G, Nigg FA, and Medema RH (2000). Polo-like kinase-1 is a target of the DNA damage checkpoint. *Nat Cell Biol* **2**, 672–676.

[24] Bassermann F, von Klitzing C, Munch S, Bai RY, Kawaguchi H, Morris SW, Peschel C, and Duyster J (2005). NIPA defines an SCF-type mammalian E3 ligase that regulates mitotic entry. *Cell* **122**, 45–57.

[25] Huang T-S, Shu C-H, Chao Y, Chen S-N, and Chen L-L (2000). Activation of MAD2 checkprotein and persistence of cyclin B1/CDC2 activity associate with paclitaxel-induced apoptosis in human nasopharyngeal carcinoma cells. *Apoptosis* **5**, 235–241.

[26] Taylor WR and Stark GR (2001). Regulation of the G2/M transition by p53. *Oncogene* **20**, 1803–1815.

[27] Bunz F, Dutriaux A, Lengauer C, Walkman T, Zhou S, Brown JP, Sedivy JM, Kinzler KW, and Vogelstein B (1998). Requirement for p53 and p21 to sustain G2 arrest after DNA damage. *Science* **82**, 1497–1501.

[28] Griffith TD and Tolmach LJ (1976). Lethal response of HeLa cells to X-irradiation in the latter part of the generation cycle. *Biophys J* **16**, 303–318.